

Activation and de-activation of fluorine synthons by nitrogen substitution in fluorinated aza-distyrylbenzenes†

Alain Collas, Roeland De Borger, Tatyana Amanova and Frank Blockhuys*

Received 18th June 2010, Accepted 10th September 2010

DOI: 10.1039/c0ce00319k

Three derivatives of *E,E*-1,4-bis[2-(2,3,4,5,6-pentafluorophenyl)ethenyl]benzene, two of which bear nitrogen atoms in the ethenyl spacers, while in a third the central benzene ring is replaced by a pyrazine moiety, have been synthesized. The supramolecular structures of the resulting set of four compounds have been studied using single-crystal X-ray diffraction to gauge the influence of the position of the nitrogen atoms on the organisation of the molecules in the solid state. The crystal packing patterns were analyzed in terms of intermolecular interactions involving the fluorine and nitrogen atoms, *i.e.*, CH \cdots F, F \cdots F, F \cdots π and CH \cdots N interactions. The analysis shows that in two of the three solid-state structures the main effect of the nitrogen atoms is an indirect one: they do not participate in intermolecular contacts themselves, but activate nearby hydrogen atoms and phenyl rings in fluorine synthons to form new interactions.

1 Introduction

Within the class of oligomeric or low-molecular-weight organic semiconductors distyrylbenzenes (DSBs) and their derivatives enjoy a great deal of interest as new materials for opto-electronic applications such as organic light-emitting diodes (OLEDs),^{1–6} gas- and ion-selective sensors,^{7,8} organic memories and non-linear optics (NLOs).^{9,10} Since these applications are invariably based on the organic materials in their solid state, it is clear that apart from their molecular properties, their bulk properties are of great importance. In turn, these bulk properties depend on the three-dimensional organization of the molecules in the solid or the crystal. Consequently, understanding and manipulating the crystal structures of organic materials such as DSBs become a central issue.

A large number of solid-state structures of DSBs have already been reported¹¹ but relatively few studies have been devoted to a systematic description of the supramolecular organisation of the molecules in terms of the presence and position of different substituents. In this context we refer to the work by Renak *et al.* who studied the crystal structures of a number of fluorinated distyrylbenzene derivatives, amongst which *E,E*-1,4-bis[2-(2,3,4,5,6-pentafluorophenyl)ethenyl]benzene (**1**, Fig. 1), and confirmed that fluorine synthons such as CH \cdots F interactions and the vertical stacking of aromatic rings are the main factors determining the observed packing.¹² Equally, our own work on methoxy-substituted DSBs^{13–16} led to insight into the occurrence and relative importance of the different types of inter- and intramolecular interactions that determine the crystal packing and which are available for methoxy groups, such as inter- and intramolecular CH \cdots O interactions and CH \cdots π contacts.

Whether it be methoxy groups or fluorine atoms, strong intermolecular interactions can only be obtained when heteroatoms (and, consequently, increased polarisation) are introduced into the molecular structures of (apolar) organic conjugated systems. Apart from doing this through the introduction of substituents containing heteroatoms *on* the carbon backbone, an alternative approach is based on the substitution of the atoms *in* the carbon backbone by heteroatoms. Considering that nitrogen is the most straightforward choice—the isoelectronic substitution of a methine (CH) group by a nitrogen atom maintains the conjugated system—a number of interesting results have been presented by Ojala *et al.* who used nitrogen atoms in the –CH=CH– spacers in DSBs to prepare benzylidene anilines with –N=CH– or –CH=N– spacers (so-called “bridge-flipped” isomers).^{17,18} The nitrogen atoms in these systems seem to have a twofold effect: (1) either they are themselves, through their lone pairs, directly involved in new intermolecular contacts (*e.g.*, strong hydrogen bonds^{19,20} or interactions with halogen atoms^{21,22}), or (2) they are *not* directly involved in new contacts, but *indirectly* generate new intermolecular contacts by altering the electron distribution within the carbon backbone, thereby activating certain atoms to engage in these new contacts.

Based on this, we became interested in the combination of the above mentioned fluorine synthons with the possibilities of new intermolecular contacts due to nitrogen atoms present *in* the backbone, not only in the ethenyl spacers of the original DSBs but also in the (central) benzene ring, and in studying how the nitrogen atoms interact with the fluorine synthons. To do this, three aza-derivatives of the above mentioned decafluoro-DSB (**1**) were synthesized and their solid-state structures were investigated. Fig. 1 presents these three additional compounds: two of them, *E,E*-1,4-bis[2-(2,3,4,5,6-pentafluorophenyl)-2-azaethenyl]benzene (**2**) and *E,E*-*N,N'*-bis(2,3,4,5,6-pentafluorobenzylidene)-1,4-phenylenediamine (**3**), bear the two nitrogen atoms in the spacers between the phenyl rings, while in the third, *E,E*-2,5-bis[2-(2,3,4,5,6-pentafluorophenyl)ethenyl]pyrazine (**4**), the nitrogen atoms are located in the central

Department of Chemistry, University of Antwerp, Universiteitsplein 1, B-2610 Wilrijk, Belgium. E-mail: frank.blockhuys@ua.ac.be; Fax: +32 3 820 23 10

† CCDC reference numbers 781116–781118. For crystallographic data in CIF or other electronic format see DOI: 10.1039/c0ce00319k

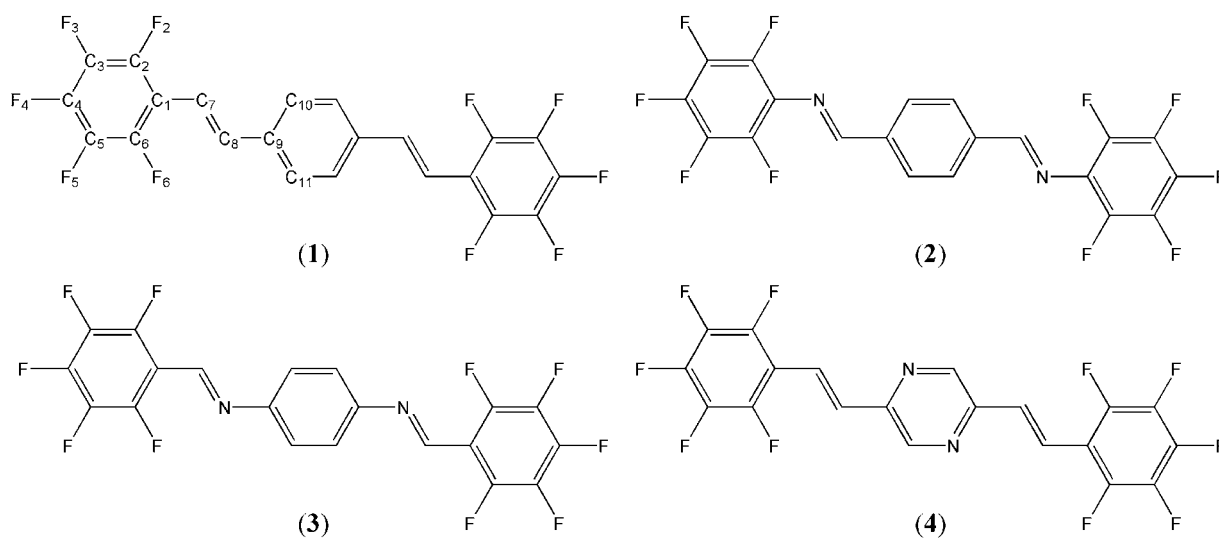


Fig. 1 The parent DSB (**1**) and its three aza-derivatives (**2–4**) under investigation. The structural formula of **1** presents the numbering scheme of the four compounds; in **2**, **3** and **4** N1 replaces C7, C8 and C10, respectively.

aromatic ring. Their experimental molecular and crystal structures were determined using XRD and the solid-state packings were analyzed. Crystal packing effects were evaluated through a comparison of the experimental solid-state molecular structures with gas-phase structures obtained from quantum chemical calculations at the DFT/B3LYP level of theory. The nitrogen atoms located in the central ring in **4** actively participate in intermolecular contacts, while those in the spacers do not. They do, however, influence the charge distribution in the backbone to such an extent that certain fluorine synthons are activated and/or de-activated.

2 Results and discussion

Compounds **2–4** were prepared by standard methods and completely characterised; note that compounds **2** and **3** are known but remained uncharacterised until now.²³ Details of the data collection and structural refinement of compounds **2–4** are collected in Table 1. The necessary data for the 158 K structure of compound **1** were obtained from the CSD²⁴ (ref. code SER-QUB²⁵). For all compounds the carbon–hydrogen distances were normalized to 1.083 Å after the refinement and the resulting geometrical parameters have been used in the following discussion of the different intermolecular short contacts. The details of these contacts have been summarized in Table 2.

Per- or polyfluorinated aromatic rings and other supramolecular synthons that introduce fluorine atoms into the molecular structure of organic molecules have proven to be excellent tools for the manipulation of the crystal structure, through specific intermolecular interactions involving the fluorine atoms.²⁶ Generally, these interactions can be subdivided into five different types (Fig. 2). The arene-perfluoroarene stacking synthon (type I), based on the interaction between an electron-poor per- or polyfluorinated phenyl ring and an electron-rich (substituted) phenyl ring, has been used extensively to achieve organization in the solid state.^{27–30} On the other hand, an electron-poor (substituted) phenyl ring can act as an electron acceptor in an

interaction with a fluorine atom (type II). Consequently, a fluorine atom can act as the electron donor in an interaction with an electron-poor per- or polyfluorinated phenyl ring (type III). Type IV contacts can be observed even when a single fluorine atom is present in the molecular structure: type IVa describes a weak hydrogen bond with a fluorine atom as acceptor, while type IVb describes the controversial F...F contacts. Solid-state NMR measurements and charge-density studies³¹ have been performed in an attempt to ascertain whether the latter are stabilizing interactions or rather caused by close packing,³² but it is not always clear what their precise nature is. The supramolecular structures of the four compounds under investigation will be described in terms of these five types.

2.1 *E,E*-1,4-Bis[2-(2,3,4,5,6-pentafluorophenyl)ethenyl]benzene (**1**)

Compound **1** crystallizes in the centrosymmetric space group $P2_1/c$.²⁵ As can be seen in the packing diagram shown in Fig. 3, the molecules adopt the *anti* conformation in which the two ethenyl spacers are oriented in opposite directions with respect to the central phenyl ring: the results of quantum chemical calculations at the DFT/B3LYP level of theory confirm that this conformer is slightly more stable (0.42 kJ mol⁻¹) than the *syn* conformation, with the two ethenyl spacers oriented in the same direction. The three benzene rings and two ethenyl spacers in **1** are all virtually co-planar, with dihedral angles about the C1–C7 and C8–C9 bonds of about 3° and 2°, respectively (Table 3). Thus, the molecular structure in the crystal is very similar to the one found in the gas phase, which has C_{2h} symmetry.

Fig. 3 shows that in one direction the molecules organise themselves side by side in a ribbon through two type IVa contacts, *i.e.*, the two weak hydrogen bonds C10–H10...F6 and C7–H7...F5, and one type IVb contact involving F2 and F5. These ribbons are then connected into layers *via* two type IVb contacts involving the two remaining fluorine atoms, F3 and F4. Finally, these layers are organised into the three-dimensional structure through one type III interaction, in which F4 contacts

Table 1 Details of the data collection and structural refinement of **2–4**

Crystal data	2	3	4
Chemical formula	C ₂₀ H ₆ F ₁₀ N ₂	C ₂₀ H ₆ F ₁₀ N ₂	C ₂₀ H ₆ F ₁₀ N ₂
Chemical formula weight/g mol ⁻¹	464.27	464.27	464.27
Cell setting	Monoclinic	Triclinic	Monoclinic
Space group	<i>P</i> 2 ₁ / <i>c</i>	<i>P</i> 1	<i>P</i> 2 ₁ / <i>c</i>
Monochromator	Graphite	Graphite	Graphite
Crystal form	Plate	Prism	Plate
Crystal size/mm	0.18 × 0.33 × 0.24	0.27 × 0.27 × 0.27	0.21 × 0.21 × 0.21
Crystal colour	Yellow	Orange	Yellow
No. of reflections for cell param.	25	25	25
θ Range/°	6.36–10.23	6.00–14.22	5.03–13.01
<i>F</i> (0 0 0)	460	230	716
<i>T</i> /K	293	293	293
<i>a</i> /Å	4.871(2)	5.846(2)	6.223(2)
<i>b</i> /Å	6.3980(10)	7.929(2)	5.9070(10)
<i>c</i> /Å	28.420(6)	10.331(3)	24.427(8)
α /°	90	109.78(2)	90
β /°	96.57(2)	102.35(3)	103.80(3)
γ /°	90	96.13(3)	90
<i>V</i> /Å ³	879.9(4)	431.8(2)	872.0(4)
<i>Z</i>	2	1	2
<i>D_x</i> /Mg m ⁻³	1.752	1.785	1.768
μ /mm ⁻¹	0.179	0.182	0.181
Data collection method	$\omega/2\theta$ scans	$\omega/2\theta$ scans	$\omega/2\theta$ scans
No. of measured reflections	3389	2612	3326
No. of independent reflections	1582	1571	1598
No. of observed reflections [<i>I</i> > 2 σ (<i>I</i>)]	1108	1219	778
θ_{\max} /°	25.32	25.32	25.33
Range of <i>h</i>	0 ≤ <i>h</i> ≤ 5	-7 ≤ <i>h</i> ≤ 3	0 ≤ <i>h</i> ≤ 7
Range of <i>k</i>	-7 ≤ <i>k</i> ≤ 7	-9 ≤ <i>k</i> ≤ 9	-7 ≤ <i>k</i> ≤ 7
Range of <i>l</i>	-32 ≤ <i>l</i> ≤ 30	-12 ≤ <i>l</i> ≤ 12	-29 ≤ <i>l</i> ≤ 28
No. of standard reflections	3	3	3
Frequency of standard reflections/ <i>h</i>	1	1	1
Intensity decay (%)	-1	27	19
Refinement on	<i>F</i> ²	<i>F</i> ²	<i>F</i> ²
GoOF	1.005	1.047	1.043
<i>R_w</i>	0.0963	0.1696	0.1738
<i>R_u</i>	0.0331	0.0562	0.0562
<i>R_{all}</i>	0.0591	0.0701	0.1477
No. of reflections used in refinement	1582	1571	1598
No. of parameters used	145	145	148
Weighting scheme	$w = 1/[\sigma^2(F_o^2) + (AP)^2 + BP]$ where $P = (F_o^2 + 2F_c^2)/3$		
A	0.0427	0.1172	0.0827
B	0.2496	0.0231	0.00
(Δ/σ) _{max}	0.00	0.00	0.00
$\Delta\rho_{\max}$	0.141	0.255	0.274
$\Delta\rho_{\min}$	-0.133	-0.267	-0.294

the centroid of a pentafluorophenyl ring, Cg(Ar_F), and one type IVb interaction involving F2 and F5 (not shown in Fig. 3). Note that all fluorine atoms of **1** are involved in intermolecular contacts.

2.2 *E,E*-1,4-Bis[2-(2,3,4,5,6-pentafluorophenyl)-2-azaethenyl]benzene (**2**)

Likewise, compound **2** crystallizes in the centrosymmetric space group *P*2₁/*c*; the packing diagrams are presented in Fig. 4. The molecules also adopt the *anti* conformation but they clearly deviate from planarity: even though the C=N spacers remain coplanar with the central ring (the torsion angle about the C8–C9 bond is limited to about 4°), the peripheral rings have now twisted out of this plane by more than 40° (Table 3). This

molecular geometry is also clearly reflected in the calculated structure which indicates torsion angles of 0.8° and 38.6°, respectively, for the molecule in *C*₂ symmetry. The increased out-of-plane twist of the peripheral rings is solely due to the presence of the nitrogen atoms and seems to be unrelated to the presence of the fluorine atoms. Indeed, in the non-fluorinated derivative *E,E*-1,4-bis(2-phenyl-2-azaethenyl)benzene the corresponding torsion angles are 39.0° and 2.6°, *i.e.*, the fluorine atoms do not introduce additional steric hindrance leading to a further out-of-plane twist.

As can be seen in Fig. 4a, the molecules are organised in layers due to two type IV intermolecular contacts. The ribbons seen in Fig. 4a are generated through contacts involving the relatively acidic hydrogen atom on the spacer (H8) and F2 in the [0 1 0] direction to form the only weak hydrogen bond (type IVa)

Table 2 Details (distances d in Å, angles θ in degrees, symmetry codes and type) of the short intermolecular contacts D–X···A given in the text; the lack of an esd on a number of the parameters is due to the normalisation of the CH distances for **2–4** and to the absence of esds in the CIF of **1**

	D	X	A	d	θ	Symmetry code	Type
1	C10	H10	F6	2.54	119	$1 + x, 1 + y, z$	IVa
	C7	H7	F5	2.58	153	$1 + x, 1 + y, z$	IVa
	C2	F2	F5	2.814	140.2	$1 + x, 1 + y, z$	IVb
	C3	F3	F4	2.811	138.7	$-1 - x, 1/2 + y, 1/2 - z$	IVb
	C4	F4	F3	2.811	171.5	$-1 - x, -1/2 + y, 1/2 - z$	IVb
	C4	F4	Cg(Ar _F)	3.431	103.0	$-1 + x, y, z$	III
	C2	F2	F5	2.900	90.6	$x, 1 + y, z$	IVb
2	C8	H8	F2	2.39	159	$x, 1 + y, z$	IVa
	C4	F4	F5	2.847(2)	168.29(14)	$-2 - x, 1/2 + y, -1/2 - z$	IVb
	C5	F5	F4	2.847(2)	137.41(13)	$-2 - x, -1/2 + y, -1/2 - z$	IVb
	C4	F4	Cg(Ar _F)	3.502(2)	102.61(12)	$-1 + x, y, z$	III
	C3	F3	F6	2.831(2)	154.24(14)	$-1 + x, 1 + y, z$	IVb
3	C7	H7	F5	2.62	163	$x, -1 + y, z$	IVa
	C10	H10	F5	2.56	120	$x, -1 + y, z$	IVa
	C10	H10	F6	2.62	120	$x, -1 + y, z$	IVa
	C11	H11	F6	2.47	170	$x, 1 - y, 1 - z$	IVa
	C2	F2	F5	2.899(2)	142.76(13)	$x, -1 + y, z$	IVb
	C5	F5	Cg(Ar _H)	3.333(2)	104.22(13)	$1 + x, 1 + y, z$	II
	C5	F5	Cg(Ar _H)	3.333(2)	104.22(13)	$1 - x, 1 - y, 1 - z$	II
4	C11	H11	N1	2.60	149	$-x, 1 - y, -z$	—
	C2	F2	F6	2.912(4)	95.97(21)	$x, -1 + y, z$	IVb
	C4	F4	F5	2.809(4)	160.8(3)	$3 - x, -1/2 + y, 1/2 - z$	IVb
	C5	F5	F4	2.809(4)	130.9(3)	$3 - x, 1/2 + y, 1/2 - z$	IVb
	C5	F5	Cg(Ar _F)	3.150(3)	132.3(2)	$2 - x, 1/2 + y, 1/2 - z$	III

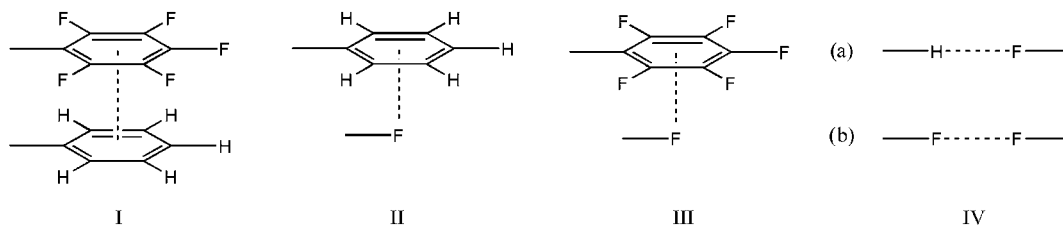


Fig. 2 The five different types of intermolecular interactions involving fluorine atoms.

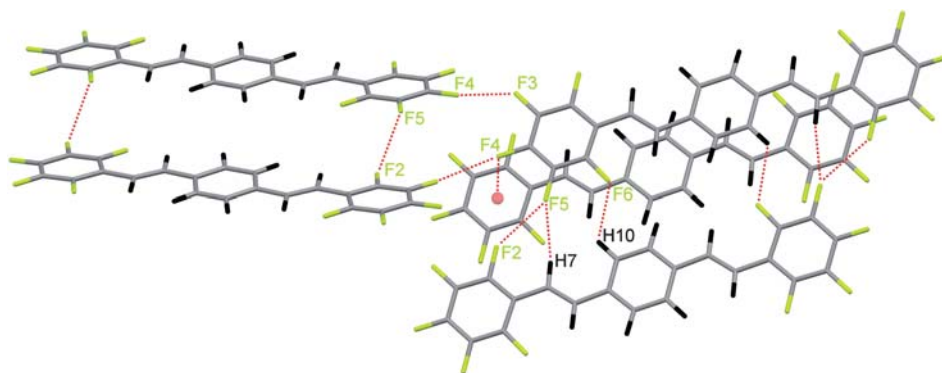


Fig. 3 View of the packing of **1** showing the CH···F and F···F contacts within the ribbons and layers and the F···Cg(Ar_F) contacts between the layers. See text for details.

present in the supramolecular structure. Within the layer, these ribbons are connected through two type IVb contacts involving the fluorine atoms in the 4- and 5-positions. Between these layers, the fluorine atoms in the 4-position contact the centroids of a fluorinated aromatic ring in an F···Cg(Ar_F) (type III) contact, which is accompanied by another type IVb contact between F3 and F6 (Fig. 4b).

2.3 *E,E*-*N,N'*-Bis(2,3,4,5,6-pentafluorobenzylidene)-1,4-phenylenediamine (**3**)

Compound **3** crystallizes in the centrosymmetric $P\bar{1}$ space group. The packing diagram is presented in Fig. 5. Similar to the conformations of **1** and **2**, the molecules of **3** are found in the *anti* conformation and the calculations predict a molecular

Table 3 Selected geometrical data for compounds **1–4**; calculated (DFT) and experimental (XRD) torsion angles in degrees

	Parameter	DFT	XRD
1	C6–C1–C7–C8	0.0	3.21
	C7–C8–C9–C10	0.0	2.24
2	C6–C1–N1–C8	38.6	42.2(3)
	N1–C8–C9–C10	0.8	4.2(3)
3	C6–C1–C7–N1	5.1	10.8(3)
	C7–N1–C9–C10	35.5	11.8(2)
4	C6–C1–C7–C8	0.0	19.6(6)
	C7–C8–C9–C10	0.0	7.2(4)

conformation with C_2 symmetry similar to the one found for **2** (Table 3), but, since the nitrogen atoms have moved to the central ring, the latter is now twisted by about 36° out of the plane formed by the C=N spacer and the peripheral ring (the torsion angle about the C1–C7 bond is limited to about 5°). Again, this particular molecular conformation is not related to the presence or absence of the fluorine atoms: in the non-fluorinated derivative *E,E*-*N,N'*-dibenzylidene-1,4-phenylenediamine the corresponding torsion angles are 1.8° and 36.5° . However, this is not what is observed in the solid state: the experimental conformation is much more planar, as the two relevant torsion angles have been reduced to about 12° and 11° , respectively (Table 3).

As can be seen in Fig. 5, the virtually planar molecules are arranged in layers (represented by the three central molecules in

Fig. 5) and within these layers four different interactions can be distinguished in the form of two bifurcated type IVa hydrogen bonds involving F5 and F6 of one molecule and the two hydrogen atoms on the central phenyl ring (H10 and H11) and the one on the C=N spacer (H7) of the next. In addition to these, there is a single type IVb contact involving F2 and F5. These layers are then connected *via* $F\cdots Cg(Ar_H)$ intermolecular contacts (type II) with the layers above and below (represented by the uppermost and lowermost molecules in Fig. 5, respectively).

2.4 *E,E*-2,5-Bis[2-(2,3,4,5,6-pentafluorophenyl)ethenyl]pyrazine (**4**)

Compound **4** crystallizes in the centrosymmetric space group $P2_1/c$. Fig. 6 displays the packing schemes. In principle, two *anti* conformers with C_{2h} symmetry are possible for compound **4**: one in which the N \cdots N axis in the central ring is aligned with the orientations of the ethenyl links, and a second in which it is not. The former, which is found in the solid state, is the more stable conformer by 14.81 kJ mol^{-1} . The corresponding value for the non-fluorinated derivative *E,E*-2,5-bis(2-phenylethenyl)pyrazine is 9.45 kJ mol^{-1} and this indicates that the fluorine atoms shift the equilibrium more in favour of the experimentally observed conformer. When incorporated into the supramolecular structure the planar gas-phase structure is distorted: the central ring remains almost coplanar with the ethenyl spacers (the torsion angle about the C8–C9 bond is limited to about 7°), but the

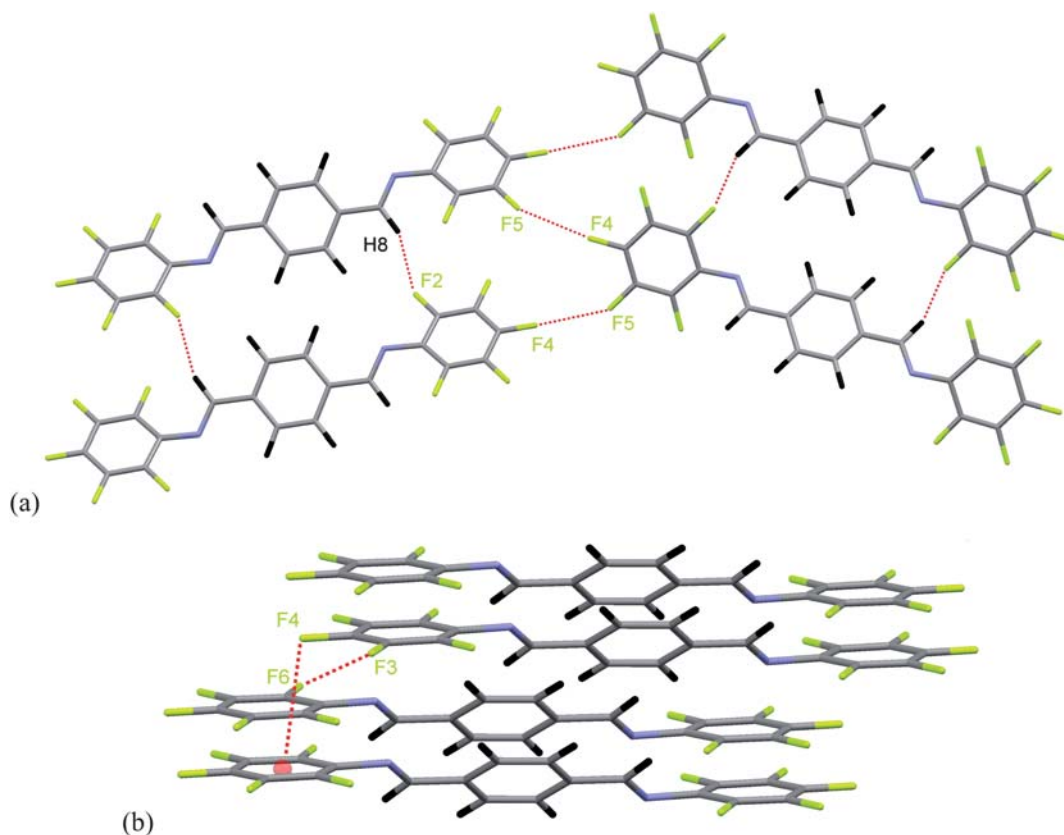


Fig. 4 View of the packing of **2** showing: (a) the CH \cdots F and F \cdots F contacts within the layer and (b) the F \cdots Cg(Ar $_F$) contacts responsible for the organisation of these layers.

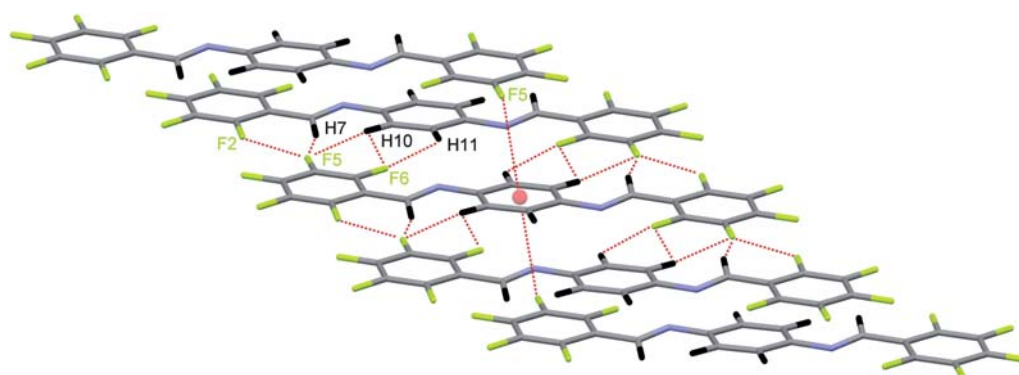


Fig. 5 View of the packing of **3** showing the CH...F and F...F contacts within the ribbons, as well as the F...Cg(Ar_H) contacts between them. See text for details.

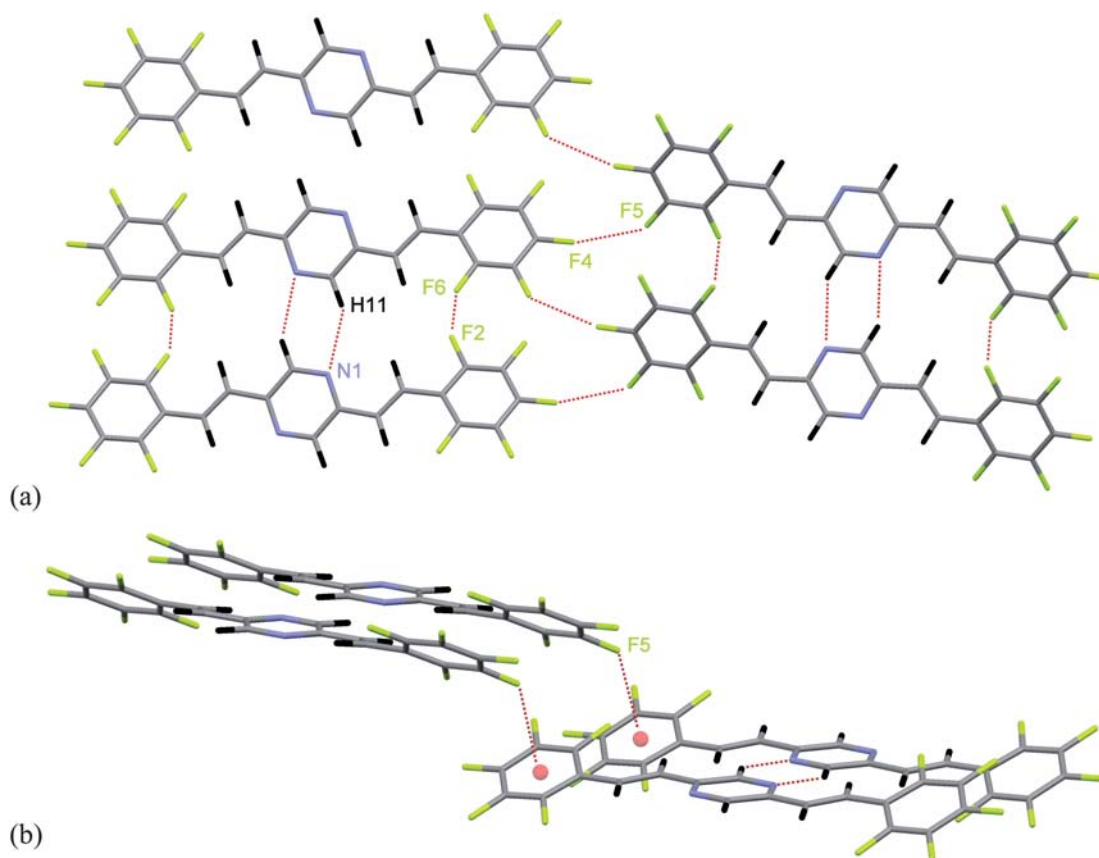


Fig. 6 View of the packing of **4** showing: (a) the CH...N dimers forming the ribbons and the F...F contacts between the ribbons and (b) the F...Cg(Ar_F) contacts responsible for the three-dimensional packing. See text for details.

peripheral rings are twisted to a somewhat larger extent, with a torsion angle about the C1–C7 bond of about 20°.

From Fig. 6 it is clear that this compound displays the CH...N weak hydrogen bond dimers typical for pyrazine derivatives, through which the different molecules organise themselves in flat ribbons in the [0 1 0] direction. In addition to these CH...N interactions, there is also a short type IVb contact involving the fluorine atoms in the 2- and 6-positions. Adjacent ribbons are connected *via* two type IVb contacts involving the fluorine atoms in the 4- and 5-positions. Finally, the observed three-dimensional

organisation is due to an F...Cg(Ar_F) contact (type III) involving F5.

2.5 The supramolecular structures of fluorinated (aza) distyrylbenzenes

The supramolecular structures of these compounds can now be compared to gauge the influence of the position of the nitrogen atoms. Due to the presence of the ten fluorine atoms on the peripheral rings the molecules of compound **1** are highly

polarized and comprise electron-poor peripheral rings and an electron-rich central ring. This is reflected in the fact that the bulk of the interactions observed in the solid state involve all five fluorine atoms on these peripheral rings. One of the hydrogen atoms on the central ring and one on the spacers become involved in two weak hydrogen bonds, but the two remaining hydrogen atoms (H8 and H11) are not used.

When nitrogen atoms are introduced in the 2-positions of the ethenyl spacers (compound **2**), the peripheral rings become even more electron-poor than in **1** due to the inductively accepting $-I$ effect of the nitrogen atom, resulting in a further polarization of the molecule. As a result, the central ring does not participate anymore in intermolecular contacts and the corresponding $\text{CH}\cdots\text{F}$ (type IVa) synthon is de-activated. All five fluorine atoms of the peripheral rings continue to be involved in the intermolecular network and they generate four of the five observed short contacts ($\text{F}\cdots\text{F}$ and $\text{F}\cdots\pi$). The fifth, a single weak hydrogen bond, is a result of the further activation of the one remaining hydrogen atom on the spacer and its corresponding $\text{CH}\cdots\text{F}$ (type IVa) synthon.

Shifting the nitrogen atom towards the central ring in compound **3** reshuffles the electron distribution throughout the carbon backbone and now the central ring becomes considerably electron-poorer than in **1**. This leads to three effects. First, the peripheral rings lose part of the activation they enjoyed in **2**, due to the absence of the nitrogen atom: only three of the five fluorine atoms on these rings are involved in intermolecular contacts, and just one $\text{F}\cdots\text{F}$ (type IVb) and no $\text{F}\cdots\pi_{\text{F}}$ (type III) contacts remain. Secondly, as in **2**, a single weak hydrogen bond, the result of the further activation of the one remaining hydrogen atom on the spacer and its corresponding $\text{CH}\cdots\text{F}$ (type IVa) synthon, is observed. Thirdly, the fact that the central ring has become more electron-poor leads to the activation of three $\text{CH}\cdots\text{F}$ (type IVa) synthons and two type II synthons, with the central ring being contacted from below and above. In effect, moving the nitrogen from the 2- to the 1-position in the ethenyl spacer has switched off the type III contact in **2** and switched on the type II contacts in **3**. Apparently, in order to maximize the number of weak $\text{CH}\cdots\text{F}$ hydrogen bonds the non-planar molecular structure of the isolated molecule has to become more planar, but this is achieved without too great a destabilization.³³

Finally, in the solid-state structure of compound **4** the $\text{CH}\cdots\text{N}$ interactions typical for pyrazine derivatives dominate the structure, but, since they are relatively short, stacking the planar conformation found for the isolated molecule would lead to intermolecular repulsion between the fluorine atoms on the peripheral rings. Therefore, a part of the stabilization associated with the planar structure is sacrificed to accommodate the perfluorophenyl rings and the latter are twisted out of the molecular plane. Once the ribbons based on the $\text{CH}\cdots\text{N}$ interactions are formed, they are organised into the three-dimensional structure *via* three $\text{F}\cdots\text{F}$ and one $\text{F}\cdots\text{Cg}$ contacts, the latter again involving the peripheral rings, as in **1**.

It is clear that nitrogen atoms in **2** and **3** do not participate directly in the interactions that determine the crystal packing: they are too well “buried” inside the backbone of the molecules to reach any other atom in a short contact. These nitrogen atoms do develop an indirect effect through “activating” the azomethine hydrogens on the spacer in **2** and **3**, as well as the central

ring in **3**, or “de-activating” the central ring in **2** and the peripheral rings in **3**. As expected, in **4** the nitrogen atoms are easily accessible and generate the typical hydrogen bonds.

The previous discussion leads to the following two conclusions. First, interactions involving hydrogen atoms ($\text{CH}\cdots\text{Y}$) are preferable over those involving only fluorine atoms. In all four structures $\text{CH}\cdots\text{Y}$ contacts can be found: for compound **4**, Y is the nitrogen atom of the pyrazine ring, while for compounds **1–3** a number of $\text{CH}\cdots\text{F}$ contacts can be observed. For all three of the latter compounds the hydrogen atom on the spacer is involved in a short $\text{CH}\cdots\text{F}$ contact, while the number of $\text{CH}\cdots\text{F}$ contacts involving the central ring is dependent on the (de)activating effect of the nitrogen atoms. Obviously, the solid-state structure of compound **4** is a clear illustration of the supremacy of the weak hydrogen bonds: the molecules are willing to give up part of their conjugative stabilization to accommodate them. On the other hand, it is also clear that, even though the weak hydrogen bonds dominate the organization of the molecules at the first level, the entire solid-state structures of these systems could not exist without the presence of the more controversial $\text{F}\cdots\text{F}$ interactions.

Secondly, it appears that these distyrylbenzenes, with their particular rod-like shape, are organised more efficiently in a three-dimensional superstructure when they are more planar. This is illustrated by the packing efficiencies of the four compounds under investigation: 75.1% (**1**@158 K), 73.6% (**1**@190 K), 71.7% (**2**), 73.1% (**3**) and 72.6% (**4**). The more planar compounds (**1** and **3**) clearly have a higher packing efficiency. Table 3 also clearly shows that compounds **1** and **3** display the largest numbers of intermolecular contacts of the four systems under investigation, which must be a direct consequence of the more favourable three-dimensional organisation.

Conspicuously absent from these solid-state structures are the typical cooperative interactions labelled type I in Fig. 2. The phenyl-perfluorophenyl stacking synthon has been used as a tool to bring about solid-state topochemical [2 + 2] photodimerisations and photopolymerizations in molecular crystals or co-crystals of stilbene-type systems.²⁵ The typical face-to-face stacking, resulting from the non-covalent interactions between the aromatic moieties, generates the necessary conditions (in particular, a distance of 3.5–4.2 Å between the ethenyl fragments) for the cycloaddition to proceed. These conditions are met in the structures of *E*-2,3,4,5,6-pentafluorostilbene²⁵ and its 4'-methyl derivative.³⁴ In these systems the ratio of the number of electron-rich phenyl rings to the number of electron-deficient perfluorophenyl rings is 1 : 1—the dependence of the occurrence of intermolecular interactions on the hydrogen–fluorine ratio has been discussed for fluorinated azines.³⁵ When this ratio is altered, such as in compounds **1–4**, in which it is 1 : 2, the $\text{Ar}_{\text{H}}\cdots\text{Ar}_{\text{F}}$ synthon is not observed. However, when aromatic solvent molecules such as *o*-xylene are incorporated into the structure of **1** (CSD ref. code SERRIQ), they can act as the missing phenyl moieties and return the ratio to 1 : 1, at which point the $\text{Ar}_{\text{H}}\cdots\text{Ar}_{\text{F}}$ synthon is again seen.²⁵

3 Experimental

3.1 Syntheses

All reagents and solvents were obtained from ACROS and used as received. Pentafluorobenzaldehyde was purchased from

Fluorochem Ltd. All NMR spectra except the ^{19}F NMR spectra were recorded in CDCl_3 with a Bruker AV-600 spectrometer at frequencies of 600.30 MHz for ^1H and 150.95 MHz for ^{13}C (broadband decoupling was applied) with tetramethylsilane (TMS) as internal standard. ^{19}F NMR spectra were recorded in CDCl_3 with a Bruker AV-300 spectrometer at a frequency of 282.40 MHz and the signals were referenced to C_6F_6 . Chemical shifts are given in ppm and coupling constants in Hz. UV/Vis absorption spectra were recorded on a Cary 5 spectrometer for solutions (about 20×10^{-6} M) of the oligomers in CH_2Cl_2 . Melting points were obtained with an open capillary electrothermal melting point apparatus and are uncorrected.

3.1.1 *E,E*-1,4-Bis[2-(2,3,4,5,6-pentafluorophenyl)-2-azaethenyl]benzene (2). A mixture of 2,3,4,5,6-pentafluoroaniline (1.8 g, 10 mmol) and terephthalic aldehyde (0.6 g, 5 mmol) in ethanol (100 ml) was refluxed overnight. After cooling, the residue was concentrated to 50 ml and the precipitated yellow product was collected by filtration and washed with cold ethanol. The yield is 196 mg (8.4%). Mp 185 °C. UV/Vis $\lambda_{\text{max}} = 332$ nm ($\log \epsilon = 4.28$). δ ^1H 8.7 (s, H8), 7.2 (s, H10 and H11). δ ^{13}C 167.2 (C8), 140.9 (C4), 139.3 (C2 and C6), 138.8 (C3 and C5), 138.6 (C9), 129.6 (C10), 126.1 (C1). δ ^{19}F 9.0 (dd, $J = 21.5$ and 6.0, F2 and F6), 2.4 (t, $J = 21.5$, F4), -1.1 (td, $J = 21.1$ and 6.0, F3 and F5). Crystals suitable for a diffraction experiment were grown by diffusion of hexane in a saturated CH_3CN solution.

3.1.2 *E,E-N,N'*-Bis(2,3,4,5,6-pentafluorobenzylidene)-1,4-phenylenediamine (3). A mixture of 2,3,4,5,6-pentafluorobenzaldehyde (2.0 g, 10 mmol) and *p*-phenylenediamine (0.6 g, 5 mmol) in ethanol (100 ml) was refluxed for 2 hours. After cooling, the orange crystals were collected by filtration and washed with cold ethanol. The yield is 1.2 g (54%). Mp 175 °C. UV/Vis $\lambda_{\text{max}} = 361$ nm ($\log \epsilon = 4.3$). δ ^1H 8.6 (s, H7), 7.3 (s, H10 and H11). δ ^{13}C 159.7 (C7), 150.3 (C9), 148.1 (C1), 143.4 (C2 and C6), 141.7 (C4), 136.9 (C3 and C5), 121.9 (C10). δ ^{19}F 20.1 (td, $J = 19.8$ and 6.4, F2 and F6), 12.5 (t, $J = 20.6$, F4), 0.4 (td, $J = 20.3$ and 6.4, F3 and F5). Crystals suitable for a diffraction experiment were grown by slow evaporation of a CHCl_3 solution.

3.1.3 *E,E*-2,5-Bis[2-(2,3,4,5,6-pentafluorophenyl)ethenyl]pyrazine (4). A mixture of 2,3,4,5,6-pentafluorobenzaldehyde (3.9 g, 20 mmol) and 2,5-dimethylpyrazine (1.1 g, 10 mmol) in DMSO (250 ml) was refluxed with ZnCl_2 for 8 hours. After cooling, the precipitated yellow product was collected by filtration and washed with cold ethanol. After refluxing for 4 hours in *p*-xylene with a catalytic amount of I_2 the pure *E,E* oligomer was filtered off and washed with cold ethanol. The yield is 2.5 g (54%). Mp 204 °C. UV/Vis $\lambda_{\text{max}} = 369$ nm ($\log \epsilon = 4.7$). δ ^1H 8.6 (s, H10), 7.7 (d, $J = 16.3$, H8), 7.5 (d, $J = 16.3$, H7). δ ^{13}C 148.9 (C9), 144.2 (C10), 141.5 (C2 and C6), 139.8 (C4), 137.0 (C3 and C5), 131.4 (C8), 128.8 (C7), 119.1 (C1). δ ^{19}F 20.1 (td, $J = 21$ and 7.3, F2 and F6), 12.5 (t, $J = 20.7$, F4), -0.4 (td, $J = 20.7$ and 7.3, F3 and F5). Crystals suitable for a diffraction experiment were grown by slow evaporation of a solution in 1,1'-dichloroethane.

3.2 X-Ray crystallography

Data collection was performed on a Enraf-Nonius Mach 3 diffractometer using Mo-K α radiation ($\lambda = 0.71073$ Å). The

CAD-4 EXPRESS³⁶ software was used for data collection and cell refinement and XCAD-4³⁷ for data reduction. The structures were solved by direct methods using SHELXS-97³⁸ and refined using SHELXL-97:³⁸ hydrogen atoms were restrained to occupy the calculated positions and defined as riding [$\text{CH} = 0.93$ Å and $U_{\text{iso}}(\text{H}) = 1.2U_{\text{eq}}(\text{C})$ for aromatic CH]. For the analysis of the supramolecular structures, CH bond lengths were normalised to the value derived from neutron diffraction (1.083 Å). After this normalisation procedure, PLATON³⁹ was used to calculate all intra- and intermolecular contacts. Figures were prepared using MERCURY (version 2.3).⁴⁰ The experimental details including the results of the refinements are given in Table 1. The numbering scheme can be found in Fig. 1.

3.3 Electrochemical measurements

Electrochemical measurements were performed using an AUTO-LAB potentiostat/galvanostat connected to a PC equipped with the "General Purpose Electrochemical System" (GPES) software. Cyclic voltammetric (CV) measurements were carried out in dry acetonitrile at 298 K under an argon atmosphere. Tetrabutylammonium tetrafluoroborate obtained from ALDRICH was used as the supporting electrolyte. Concentrations of 0.4 mM and 80 mM for the oligomer and electrolyte, respectively, were used. Extra dry acetonitrile (<50 ppm water) was purchased from ACROS and stored on 3 Å sieves. Standard voltammograms were recorded at a scan rate of $0.1 \text{ V}^{-1} \text{ s}^{-1}$ using the ferrocene/ferrocenium (Fc/Fc^+) couple as reference. The working electrode was a BASi stationary voltammetry electrode comprising a platinum electrode disc with a diameter of 3 mm. A platinum plate was used as the auxiliary electrode and a silver wire as the pseudo-reference electrode. The large number of fluorine atoms makes the oxidation of compounds **1–4** virtually impossible. Reduction potentials could not be determined due to the irreversible nature of the systems, but forward and reverse peak potentials (in V vs. Fc/Fc^+ with standard deviations between brackets), respectively, are reported for **1** [$-1.634(8)$ and $-0.958(36)$], **2** [$-1.649(21)$ and $-0.971(8)$], **3** [$-1.528(23)$ and $-1.095(51)$] and **4** [$-1.544(54)$ and $-0.987(37)$].

3.4 Quantum chemical calculations

The molecular structures of different conformers of compounds **1–4** were optimized at the DFT/B3LYP/6-31G* level of theory using the Gaussian 03 program package,⁴¹ adding diffuse functions to the nitrogen and fluorine atoms only; the basis sets were used as they are implemented in the program. Frequency calculations were performed to ascertain that the resulting structures— C_{2h} symmetry for **1** and **4**, and C_2 symmetry for **2** and **3**—are minima on the Potential Energy Surface (PES).

4 Conclusions

The crystal structures of three derivatives of *E,E*-1,4-bis[2-(2,3,4,5,6-pentafluorophenyl)ethenyl]benzene, *i.e.*, *E,E*-1,4-bis[2-(2,3,4,5,6-pentafluorophenyl)-2-azaethenyl]benzene, *E,E-N,N'*-bis(2,3,4,5,6-pentafluorobenzylidene)-1,4-phenylenediamine and *E,E*-2,5-bis[2-(2,3,4,5,6-pentafluorophenyl)ethenyl]pyrazine, have been analysed in terms of the different intermolecular interactions involving the heteroatoms. The analysis shows

that when the nitrogen atoms are not available to participate directly in intermolecular interactions (*i.e.*, when they are positioned in the spacers between the phenyl rings), they indirectly generate new contacts by activating synthons involving nearby hydrogen atoms and phenyl rings. The supramolecular structures are dominated by CH \cdots N and CH \cdots F hydrogen bonds, as a result of which additional weaker F \cdots F and F \cdots π contacts can be observed. The latter are, however, indispensable for the formation of the three-dimensional structure.

Acknowledgements

A.C. and R.D.B. wish to thank the Institute for the Promotion of Innovation by Science and Technology in Flanders (IWT) for their predoctoral grants. The authors are grateful to Dr A. Yu. Makarov (Institute of Organic Chemistry, Russian Academy of Sciences, Novosibirsk) for recording the NMR data. Financial support by FWO-Vlaanderen under grant G.0129.05 and by the University of Antwerp under Grant GOA-2404 is gratefully acknowledged. The authors gratefully acknowledge the University of Antwerp for access to the university's computer cluster CalcUA.

References

- Y. D. Jin, H. Z. Chen, P. L. Heremans, K. Aleksandrak, H. J. Geise, G. Borghs and M. Van der Auweraer, *Synth. Met.*, 2002, **127**, 155–158.
- Y. D. Jin, J. P. Yang, P. L. Heremans, M. Van der Auweraer, E. Rousseau, H. J. Geise and G. Borghs, *Chem. Phys. Lett.*, 2000, **320**, 387–392.
- F. T. Luo, Y. T. Tao, S. L. Ko, H. C. Chang and H. Chen, *J. Mater. Chem.*, 2002, **12**, 47–52.
- W. Tachelet, S. Jacobs, H. Ndayikengurukiye, H. J. Geise and J. Gruner, *Appl. Phys. Lett.*, 1994, **64**, 2364–2366.
- J. P. Yang, P. L. Heremans, R. Hoefnagels, W. Tachelet, P. Dieltiens, F. Blockhuys, H. J. Geise and G. Borghs, *Synth. Met.*, 2000, **108**, 95–100.
- J. P. Yang, Y. D. Jin, P. L. Heremans, R. Hoefnagels, P. Dieltiens, F. Blockhuys, H. J. Geise, M. Van der Auweraer and G. Borghs, *Chem. Phys. Lett.*, 2000, **325**, 251–256.
- E. Vanneste, M. De Wit, K. Eyckmans and H. J. Geise, *Semin. Food Anal.*, 1998, **3**, 107–113.
- J. N. Wilson and U. H. F. Bunz, *J. Am. Chem. Soc.*, 2005, **127**, 4124–4125.
- D. S. Chemla, *Nonlinear Optical Properties of Organic Molecules and Crystals*, Academic Press, Boston, 1987.
- R. M. Metzger, B. Chen, U. Hopfner, M. V. Lakshminantham, D. Vuillaume, T. Kawai, X. L. Wu, H. Tachibana, T. V. Hughes, H. Sakurai, J. W. Baldwin, C. Hosch, M. P. Cava, L. Brehmer and G. J. Ashwell, *J. Am. Chem. Soc.*, 1997, **119**, 10455–10466.
- A CSD search (v. 5.31, updated in May 2010) for all substituted 1,4-distyrylbenzenes resulted in 151 hits.
- M. L. Renak, G. P. Bartholomew, S. J. Wang, P. J. Ricatto, R. J. Lachicotte and G. C. Bazan, *J. Am. Chem. Soc.*, 1999, **121**, 7787–7799.
- C. M. L. Vande Velde, J. K. Baeke, H. J. Geise and F. Blockhuys, *Acta Crystallogr., Sect. C: Cryst. Struct. Commun.*, 2005, **61**, o284–o287.
- C. M. L. Vande Velde, L. J. Chen, J. K. Baeke, M. Moens, P. Dieltiens, H. J. Geise, M. Zeller, A. D. Hunter and F. Blockhuys, *Cryst. Growth Des.*, 2004, **4**, 823–830.
- C. M. L. Vande Velde, H. J. Geise and F. Blockhuys, *Acta Crystallogr., Sect. C: Cryst. Struct. Commun.*, 2004, **61**, o21–o24.
- C. M. L. Vande Velde, H. J. Geise and F. Blockhuys, *Cryst. Growth Des.*, 2006, **6**, 241–246.
- W. H. Ojala, T. M. Arola, N. Herrera, B. Balidemaj and C. R. Ojala, *Acta Crystallogr., Sect. C: Cryst. Struct. Commun.*, 2007, **63**, o207–o211.
- W. H. Ojala, J. M. Smieja, J. M. Spude, T. M. Arola, M. K. Kuspa, N. Herrera and C. R. Ojala, *Acta Crystallogr., Sect. B: Struct. Sci.*, 2007, **63**, 485–496.
- B. T. Loughrey, M. L. Williams and P. C. Healy, *Acta Crystallogr., Sect. E: Struct. Rep. Online*, 2009, **65**, o2087.
- G. Rothenberg, A. P. Downie, C. L. Raston and J. L. Scott, *J. Am. Chem. Soc.*, 2001, **123**, 8701–8708.
- M. T. Ahmet, J. Silver and A. Houlton, *Acta Crystallogr., Sect. C: Cryst. Struct. Commun.*, 1994, **50**, 1814–1818.
- J. L. Wardell, S. M. S. V. Wardell, J. M. S. Skakle, J. N. Low and C. Glidewell, *Acta Crystallogr., Sect. C: Cryst. Struct. Commun.*, 2002, **58**, o428–o430.
- G. F. D'Alelio, J. V. Crivello, R. K. Schoenig and T. F. Huemmer, *J. Macromol. Sci., Part A: Pure Appl. Chem.*, 1967, **1**, 1251–1258.
- F. H. Allen, *Acta Crystallogr., Sect. B: Struct. Sci.*, 2002, **58**, 380–388.
- G. W. Coates, A. R. Dunn, L. M. Henling, J. W. Ziller, E. B. Lobkovsky and R. H. Grubbs, *J. Am. Chem. Soc.*, 1998, **120**, 3641–3649.
- K. Reichenbacher, H. I. Suss and J. Hulliger, *Chem. Soc. Rev.*, 2005, **34**, 22–30.
- C. Y. Dai, P. Nguyen, T. B. Marder, A. J. Scott, W. Clegg and C. Viney, *Chem. Commun.*, 1999, 2493–2494.
- W. J. Feast, P. W. Lovenich, H. Puschmann and C. Taliani, *Chem. Commun.*, 2001, 505–506.
- C. E. Smith, P. S. Smith, R. L. Thomas, E. G. Robins, J. C. Collings, C. Y. Dai, A. J. Scott, S. Borwick, A. S. Batsanov, S. W. Watt, S. J. Clark, C. Viney, J. A. K. Howard, W. Clegg and T. B. Marder, *J. Mater. Chem.*, 2004, **14**, 413–420.
- S. Z. Zhu, S. F. Zhu, G. F. Jin and Z. T. Li, *Tetrahedron Lett.*, 2005, **46**, 2713–2716.
- D. Chopra, T. S. Cameron, J. D. Ferrara and T. N. G. Row, *J. Phys. Chem. A*, 2006, **110**, 10465–10477.
- A. R. Choudhury and T. N. G. Row, *Cryst. Growth Des.*, 2004, **4**, 47–52.
- J. Bernstein, Y. M. Engel and A. T. Hagler, *J. Chem. Phys.*, 1981, **75**, 2346–2353.
- CCDC 781119.
- V. R. Vangala, A. Nangia and V. M. Lynch, *Chem. Commun.*, 2002, 1304–1305.
- Enraf-Nonius, CAD-4 EXPRESS, Enraf-Nonius, Delft, The Netherlands, 1994.
- K. Harms and S. Wocadlo, XCAD4, University of Marburg, Germany, 1996.
- G. M. Sheldrick, *Acta Crystallogr., Sect. A: Found. Crystallogr.*, 2008, **64**, 112–122.
- A. L. Spek, *J. Appl. Crystallogr.*, 2003, **36**, 7–13.
- C. F. Macrae, P. R. Edgington, P. McCabe, E. Pidcock, G. P. Shields, R. Taylor, M. Towler and J. van de Streek, *J. Appl. Crystallogr.*, 2006, **39**, 453–457.
- M. J. Frisch, G. W. Trucks, H. B. Schlegel, G. E. Scuseria, M. A. Robb, J. R. Cheeseman, J. A. J. Montgomery, T. Vreven, K. N. Kudin, J. C. Burant, J. M. Millam, S. S. Iyengar, J. Tomasi, V. Barone, B. Mennucci, M. Cossi, G. Scalmani, N. Rega, G. A. Petersson, H. Nakatsuji, M. Hada, M. Ehara, K. Toyota, R. Fukuda, J. Hasegawa, M. Ishida, T. Nakajima, Y. Honda, O. Kitao, H. Nakai, M. Klene, X. Li, J. E. Knox, H. P. Hratchian, J. B. Cross, C. Adamo, J. Jaramillo, R. Gomperts, R. E. Stratmann, O. Yazyev, A. J. Austin, R. Cammi, C. Pomelli, J. W. Ochterski, P. Y. Ayala, K. Morokuma, G. A. Voth, P. Salvador, J. J. Dannenberg, V. G. Zakrzewski, S. Dapprich, A. D. Daniels, M. C. Strain, O. Farkas, D. K. Malick, A. D. Rabuck, K. Raghavachari, J. B. Foresman, J. V. Orti, Q. Cui, A. G. Baboul, S. Clifford, J. Cioslowski, B. B. Stefanov, A. L. G. Liu, P. Piskorz, I. Komaromi, R. L. Martin, D. J. Fox, T. Keith, M. A. Al-Laham, C. Y. Peng, A. Nanayakkara, M. Challacombe, P. M. W. Gil, B. Johnson, W. Chen, M. W. Wong, C. Gonzalez and J. A. Pople, Gaussian Inc., Pittsburg, PA, 2003.